Efficient Catalytic Activity of Ionic Liquid-Supported NiFe$_2$O$_4$ Magnetic Nanoparticle Doped Titanium Dioxide Nano-Composite

Vasanthakumar Arumugam, Gyanasivan G. Redhi, and Robert M. Gengan

Abstract—**In this work the author disclose an effective and environment-friendly approach to the preparation of an ionic liquid supported, magnetic nanoparticle doped titanium oxide nanocomposite. The novel ionic liquid N-(2′, 3′-epoxypropyl)-N-methyl-2- pyrrolidonium salicylate was first synthesized and characterized by ^{1}H-NMR, ^{13}C-NMR, elemental Analysis and FTIR. It was subsequently used for the preparation of a composite material by traditional protocols. This ionic liquid is able to connect the NiFe$_2$O$_4$ magnetic nanoparticles with titanium dioxide via strong ionic liquid interactions. The composite was characterized by FT-IR, Scanning Electron Microscopy (SEM), Energy Dispersive X-Ray (EDS) analysis, Transmission Electron Microscopy (TEM), High-Resolution Transmission Electron Microscopy (TEM) and Diffraction studies (DF). The catalytic activities of these composites were assessed by the reduction of nitro aniline with the aid of UV spectroscopy. Furthermore, the composite material was easily recovered and re-used with negligible loss of its catalytical activity.**

Index Terms—**Pyrrolidone, NiFe$_2$O$_4$, salicylate, epoxypropyl, nanocomposite, nitroaniline, ionic liquid.**

I. INTRODUCTION

In the last decade, many researchers have focused on nanoscale metal oxide particles and found fascinating properties for novel applications [1], [2]. Many industries such as cosmetic, pharmaceutical, textile, food-processing and printing are using dyes and pigments in their products [3], however some environmental-friendly microorganisms are affected by highly toxic dyes due to those industries discarding them illegally [3]. Generally metal nanoparticles have some extraordinary physical and chemical properties such as large specific surface area, high number of active sites, high physical, chemical and thermal stabilities, strong electron transfer abilities and high activity and efficiency; these are the properties which are extensively exploited in the degradation of dyes [4], [5].

Most of the nanoscience scientists are doing their research with TiO$_2$ due to its interesting applications in numerous fields of materials engineering, dye-sensitized cells, paint industry, sensors and chemical engineering [6], [7]. The high number of applications of TiO$_2$ is because of their strongly influenced physiochemical properties such as phase structure, surface area and crystallite size [8], [9]. Titanium dioxide is a successful material which can be applied for the functionalization of magnetic nanoparticle and coating material [10]-[13]. In recent years, researchers have developed and improved heterogeneous catalyst systems which have solid phase supported nanoparticles such as titanium dioxide (NPS), gum and Fe$_3$O$_4$ [6], [14], [15].

Ionic liquid coated titanium dioxide composites have more applications due to their enhanced chemical properties and physical nature of the material. In general important properties of the room temperature ionic liquids such as low surface tension and vapor pressure enables it to act as a stabilizer to produce lower particle growth [16]-[18], and reduce the formed nanoparticle surface area [19]. In particular, the 1-pentyl-3-methylimidazolium bromide coated titanium dioxide ([PMIM]Br@TiO$_2$) dispersed in an organic solvent surrounded by a porous membrane and supported by capillary force and sinification [20].

Applications of magnetic nanoparticles include bioimaging [21] and easily separable and recyclable of heterogeneous nanoparticle catalysts [22]. Polystyrene -magnetite mesoporous titanium dioxide nanocomposite (PS/Fe$_3$O$_4$/mTiO$_2$) was synthesized by a facile method and these have potential application in the management of pollutants in water such as cyanobacteria [23]. The degradation of methylene blue under ultraviolet light irradiation was investigated with Fe$_3$O$_4$-TiO$_2$ nanocomposite and Abbasil. At.al. confirmed the photocatalytic activity of magnetite-titanium dioxide nanocomposite [24]. NiFe$_2$O$_4$/PAMA/Ag–TiO$_2$ nanocomposite was synthesized inexpensively and eco-friendly by facile reproducible citrate-gel methodology, these composites has been used as recyclable antibacterial material. [25].

The sono-catalytic activity and good magnetism of nanocomposite gama-Fe$_2$O$_3$ and TiO$_2$ NTs/c-Fe$_2$O$_3$ have been synthesized by a facile polyol method and exploited the principle of the isoelectric point method [26]. The phases of the titanium analogue such as anatase/rutile and silicon dioxide combined to form the nanocomposite with cobalt iron magnetite (CoFe$_2$O$_4$) nanoparticle, which has highly photocatalytic activity for oxidation of methylene blue under UV light. [27] Photo degradation of phenol under UV irradiation was investigated by using photo-catalytically active iron oxide (Fe$_3$O$_4$) nanoparticle functionalized TiO$_2$.

The present work related to synthesis of the novel N-(2 ́, 3 ́-epoxypropyl)-N-methyl-2- pyrrolidonium salicylate and its use to make the nanocomposite have been shown excellent

catalytic activity which was verified by the reduction of 2-nitroaniline to 2-aminoaniline, monitored using UV-vis spectroscopy.

II. MATERIALS AND METHODS

A. Materials

N-methyl-2-pyrrolidone, epichlorohydrin, sodium salicylate, 2-nitroaniline, nickel sulphate, ferrous sulphate, ferric chloride, liquid ammonia, titanium dioxide acetonitrile, methanol, acetone, and hexane were purchased from Fluka with purity of ≥ 99%. Ultrapure deionized water was used in these experiments. The water content was found using a Metrohm Karl Fishcher coulometer to be 0.05% in $[EPPYRO]^+[SAL]^-$.

B. Synthesis of [EPPY]+[Cl]-

A 50 mL three-necked round bottom flask with a thermometer inlet over cold water flowing condenser was used. Nitrogen gas was flushed into the round bottom flask and addition of 0.1 mol of freshly distilled N-methyl-2-pyrrolidone mixed with 10 mL of acetonitrile, followed by 0.11 mol of epichlorohydrin. The mixture was brought to a moderate reflux (90-100)^{o}C, then heated under reflux for 48 hours with constant stirring and then cooled to room temperature. The volatile materials were removed under reduced pressure to give a yellow coloured ionic liquid, N-(2′, 3′-epoxypropyl)-N-methyl-2-pyrrolidonium chloride $[EPPY]^+[Cl]^-$ [28] see the scheme: 1. It was characterized by the following technique: NMR (1H and13C), elemental analysis and FTIR. Analytical data of the synthesized ionic liquid was checked by HPLC and found to be 98.1%. FTIR (v=cm^{-1}): 3442, 2995, 1621, 1501, 1403, 1332, 1256, 1113, 967, 856, 756, 679, 561, 479. $[EPPY]^+[Cl]^-$ 1H NMR (400 MHz, DMSO): δ 3.48 - 3.51 (m, 1H), 3.30 - 3.32 (t, 2H), 2.76 - 3.29 (s, 1H), 2.61 - 2.62 (s, 3H). 2.26-2.30 (d, 1H) 1.96 - 1.98 (t, 2H) 1.90 - 1.94 (m, 2H) 13C NMR (100 MHz, DMSO): δ 175.03, 51.22, 49.38, 45.72, 45.00, 30.62, 29.50, and 17.59. Elemental Analysis (in %): Theoretical calculation for: $C_8H_{14}NO_2$: C, 50.14; H, 7.36; N, 7.31. The values found (in %): C, 50.45; H, 7.10; N, 7.17.

Scheme: 1
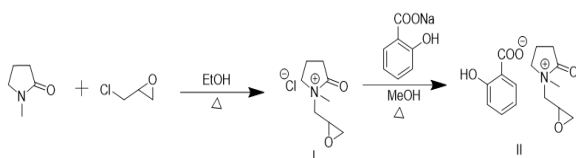
C. Synthesis of [EPPY]$^+$[SAL]$^-$

In a 50 mL round-bottomed flask, the desired quantity of sodium salicylate (0.112 mol) was dissolved in methanol to make a clear solution. Then the above synthesized intermediate ionic liquid $[EPPY]^+[Cl]^-$ was added to exchange salicylate anion. The product was purified by a solvent wash with acetone, followed by petroleum ether and hexane to remove unwanted starting materials and sodium chloride then distilled again at 80°C for 10 hrs to get pure moisture-free ILs see the scheme: 1. The $[EPPY]^+[SAL]^-$ was

characterized by the following methods: NMR (^{1}H and ^{13}C), elemental analysis and FTIR. Analytical data of the synthesized ionic liquid was checked by HPLC and found to be 98.9%. The structure of $[EPPY]^+[SAL]^-$ is as shown in FTIR (v=cm^{-1}): 3442, 2995, 1621, 1501, 1403, 1332, 1256, 1113, 967, 856, 756, 679, 561, 479.$[EPPY]^+[SAL]^-$ 1H NMR (400 MHz, DMSO): δ1.9 - 2.0(M, 2H), 2.15 - 2.3(t, 2H), 2.7 - 2.8(s, 3H), 3.3 - 3.4(m, 3H), 3.5 -3.65(d, 2H), 3.66 - 3.90(m, 1), 4.0 - 4.2(m, 1), 6.75 - 6.85(t, 1H), 6.86 - 7.00(m, 1H), 7.10 - 7.30(t, 1H), 7.40 - 7.60(m, 1H), 7.65 - 7.95(d-d, 1H). 13C NMR (100 MHz, DMSO): δ18, 30, 33, 51, 65, 72, 75, 115, 120, 122, 132, 134, 138, 163 and 178. Elemental Analysis: Theoretical calculation for: C15H21NO4: C, 64.50; H, 7.58; N, 5.01; O, 22.91. The values found: C, 64.95; H, 7.10; N, 5.28; O, 23.36.

### D. Preparation of IL/Fe$_3$O$_4$/TiO$_2$ Nanocomposite

The nickel ferrite magnetite nanoparticle was prepared according to the previous method [29], [30]. Briefly, 1.0 gram of nickel ferrite magnetic nanoparticle $NiFe_2O_4$ and N-(2´, 3´-epoxypropyl)-N-methyl-2- pyrrolidonium salicylate ionic liquid (IL) were taken separately. The ionic liquid was dissolved in ultra-pure deionized water to which the above-weighed nickel ferrite magnetic nanoparticle was added slowly at constant stirring for 24 hrs at room temperature; it was then dried at 80°C for 12 hrs to produce a dry brown powder then without purification of the material further it was dispersed in 20 mL of ultra-pure water and sonicated. Separately 2.0 gram of TiO_2 was dispersed in 20 mL water and sonicated for 15 minutes and this solution was add to above magnetic nanoparticle dispersion at constant stirring. The reaction mixture was transferred to round bottomed flask and placed in a temperature controlled oil bath with a magnetic stirrer. The temperature of the reaction was maintained at 140°C for 16 hrs. The final product was dried under vacuum for 10 hrs to produce light brown coloured nanocomposite. It was purified by washing with ultrapure water and dispersed in ethanol. The composite was then characterized by FTIR, SEM, EDS and TEM.

III. INVESTIGATION OF CATALYTIC ACTIVITY OF NANOCOMPOSITE

The investigation of the catalytic activity of ionic liquid nickel-iron magnetite titanium dioxide nanocomposite for the reduction of 2-nitroaniline was carried out in room temperature monitoring under UV spectroscopy. In a general procedure, 2-nitroaniline (0.5 mL of 0.5 mM) was mixed with 0.5 mL of freshly prepared aqueous $NaBH_4$ solution (0.4M) and 1.95 mL of deionized water to form a deep yellow solution. Then, 0.05 mL of IL/$NiFe_2O_4$/TiO_2 nanocomposite dispersion (0.2 mg/mL) was added into the quartz cuvette. The above-mixed solution was detected by using UV-Vis spectrophotometer every ten minutes to monitor the variation of 2-nitroaniline concentration. After the solution became colorless, the IL/$NiFe_2O_4$/TiO_2 hybrid was separated from the reaction mixture under a magnetic field and it was then used for another cycle of 4-Nitroaniline (4-NA) reduction. The samples were filtered, centrifuged and their concentration was determined by UV–visible spectrometry.

IV. RESULT AND DISCUSSION

The novel synthesized nanocomposite was investigated by FT-IR spectroscopy to identify the valuable information on the shift in the stretching frequencies. The FT-IR spectra of TiO_2 and $IL/NiFe_2O_4/TiO_2$ nanocomposite are shown in Fig. 1 and 2. The peak at 3294 cm^{-1} corresponds to the OH stretching vibration of the IL. A band with medium intensity at 1252 cm^{-1} with two shoulders 1103 at and 1300 cm^{-1} corresponds to the stretching vibrations of C-O-C group and ring vibrational modes in the composition of cyclic structures was observed.
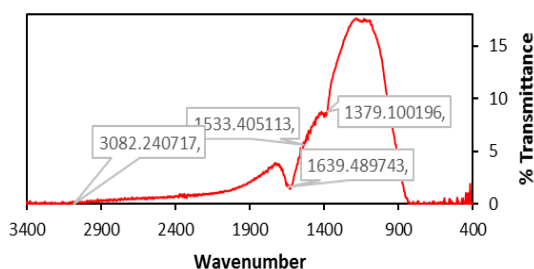
Fig. 1. FT-IR spectrum for TiO_2.
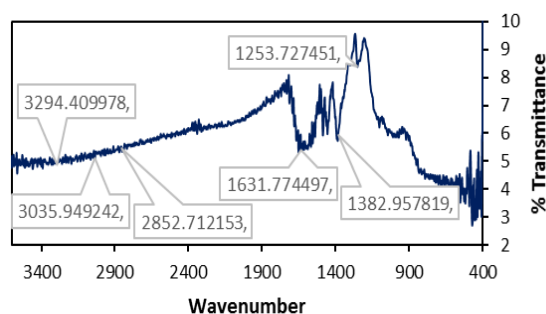
Fig. 2. FT-IR spectrum for $NiFe_2O_4/IL/TiO_2$ nanocomposite.

A broad band with low intensity arises at 1644 cm^{-1} indicates the carbonyl group nearby the amine group. The C-H aromatic stretching and bending vibrations of the IL is observed at 2997 cm^{-1} and 2344 cm^{-1}. The peak at 2850 cm^{-1} shows aliphatic C-H stretching and bending vibrations of IL. The OH stretching of the TiO_2 gives a peak at 3396 cm^{-1}. The peaks at 624 cm^{-1} and 471 cm^{-1} are attributed to Ti-O stretching mode [31], [32]; the main absorption bands at 578 cm^{-1} and 453 cm^{-1} belong to the metal–oxygen stretching vibrations of $NiFe_2O_4$ nano structures [33]. The C-O stretching vibration of the carboxylic group gives a peak at 1676 cm^{-1}. The spectrum displays a band at 3420 cm^{-1}, corresponding to the stretching mode of OH group of adsorbed hydroxyl group. The strong absorption band at 442 and 580 cm^{-1} corresponding to the $NiFe_2O_4$-TiO_2 lattice and broad absorption band at 3392 cm^{-1} are allocated to adsorbed OH group on the surface of the nanocomposite. There are no other important peaks related our nanocomposite. The peak 441 cm^{-1} could be corresponding to Ti-O stretching in rutile phase [34].These observations confirm the incorporation of $IL/NiFe_2O_4$ nanoparticle into the TiO_2 matrix

The surface morphology of the samples was observed by SEM (Fig. 1); the highly agglomerated porous foam-like structure of $NiFe_2O_4$, TiO_2 and IL, which is characteristic of the synthesized composite is observed in contrast to the bare $NiFe_2O_4$. The nanoscale crystallites could be noticeably

distinguished from the SEM image of TiO_2 and $NiFe_2O_4/TiO_2$ nanocomposites. The $NiFe_2O_4$ nanoparticles are bonded or capped with IL to form the intermediate composite and the intermediate composite mixture was combined with titanium dioxide matrix that's why it showed cluster like images. Also, the $NiFe_2O_4$ nanoparticles with the average particle size around 150 nm dispersed on synthesized nanocomposites is observable. The SEM picture also reveals that the doping of $NiFe_2O_4$ magnetite nanoparticles has increased the surface area of the catalyst surface.
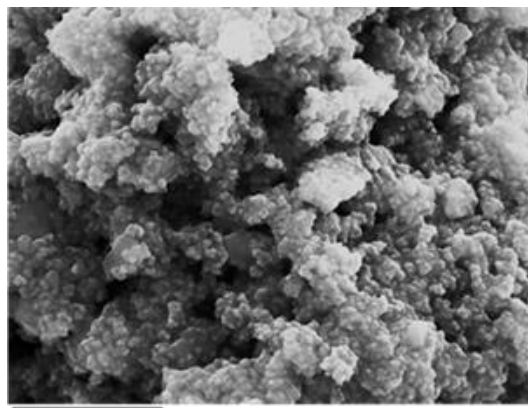
Fig. 3. SEM image of $NiFe_2O_4/IL/TiO_2$ nanocomposite.

The SEM image indicates (Fig. 3) that the spreading of $NiFe_2O_4$ on the surface of titanium dioxide is not uniform and the $NiFe_2O_4/IL/TiO_2$ catalyst contains irregularly shaped particles which may be due to the aggregation of ionic liquid and tiny crystals magnetic nanoparticles. The actual percentage of the elements in the composites was confirmed by energy dispersive spectroscopy [EDS] analysis. The identification of the elements from EDS spectra indicates the presence of Iron (4.46%), titanium (33.05%) oxygen (46.21%), carbon (14.76%) and nickel (1.51%) (Table I) which explains that the composite has been confirmed. Then EDS image (Fig. 4 and Table I) displays the percentage of all elements such as Ni, Fe, Ti, C, O except nitrogen due to the ionic liquids binding with the inner layer of titanium oxide and the percentage of the nitrogen is also low. The colouring map shows (Fig. 5) the presence of nitrogen but the EDS indicates zero percentage. The EDS only indicates the presence of ILs in composite via the presence of the C, O and N. The morphology of the resultant $NiFe_2O_4/IL/TiO_2$ nanocomposites was investigated.
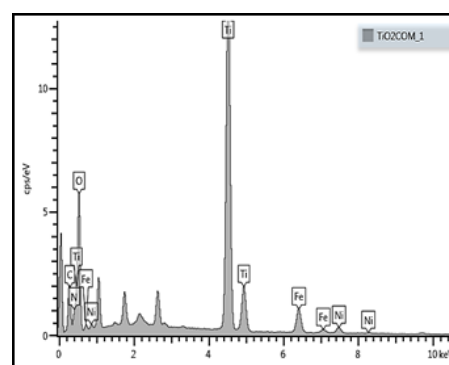
Fig. 4. EDS image of $NiFe_2O_4/IL/TiO_2$ nanocomposite.

TEM image of the resulting $NiFe_2O_4/IL/TiO_2$

nanocomposite clearly indicates that the surface was covered by IL, $NiFe_2O_4$ nanoparticle on titanium dioxide. Morphology of the synthesized nanocomposites was examined by TEM as shown in Fig. 6. The nickel-iron magnetic nanoparticles have been a cubic unit cell with both octahedral and tetrahedral.
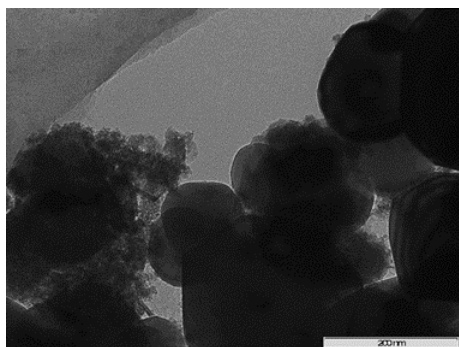
TABLE I: EDS COMPOSITION FOR $NiFe_2O_4$/IL/TiO_2 NANOCOMPOSITE

TiO_2COM	Wt%	Wt% Sigma
C	14.76	0.33
N	0	0
O	46.21	0.39
Ti	33.05	0.26
Fe	4.46	0.09
Ni	1.51	0.08
Total	100	

Fig. 5. EDS colouring map for $NiFe_2O_4$/IL/TiO_2 nanocomposite.

Co-ordinated Fe^{3+} and Ni^{2+}. A typical high-resolution TEM image Fig. 7 display the lattice fringes with a spacing 0.51 nm; the average of these synthesized nanoparticles is about 30 nm. The diameter of the magnetite nanoparticle was increased when the temperature increased from 100 to 300°C. The above results clearly explain the growth of the $NiFe_2O_4$ catalyst during thermal treatment [35]. The formation of $NiFe_2O_4$/IL/TiO_2 nanocomposite was further analyzed by low and high magnification to identify the clear structure and crystallinity of nanoparticles.

TEM images of the nanocomposites also expose the nickel iron nanoparticle with ionic liquid was decorated in TiO_2. The HRTEM image shows (Fig. 7) the crystal lattice of the nickel-iron nanoparticles. Furthermore, to the characteristic diffraction peaks (Fig. 8) correspond to $NiFe_2O_4$ and TiO_2.

Fig. 6. TEM image of $NiFe_2O_4$/IL/TiO_2 nanocomposite.

The reduction and oxidation properties of TiO_2 nanocomposite are dependent on the negative conduction or positive valence band; more negative bands could be the reason for high reducing power, and high oxidation occurs due to the greater positive valence band in nature. Compatible band configuration and contact among $NiFe_2O_4$ and TiO_2 could extend the lifetime and stimulate spatial separation of generated charge carriers. Interestingly the catalytic performance of $NiFe_2O_4$/IL/TiO_2 nanocomposites might depend on the enhanced synergistic effect of the high reducing capability of TiO_2 and IL, exhaustive absorbance at the long wavelength light by $NiFe_2O_4$ particles, at preferred fractions of two kinds of IL and NPS materials. The appropriate amount of $NiFe_2O_4$ could act as a linker for an electron to increase the effectiveness of charge separation and inhibit the recombination of electrons and holes [36]. The catalytic activity of the Ni ferrite ionic liquid TiO_2 nanocomposite was investigated by monitoring the reduction of 2-nitroaniline in the presence of $NaBH_4$ in an aqueous solution, at room temperature. The synthesized composite is a good medium for electron transfer of BH_4 ions and the reaction was checked by recording of time-dependent UV-vis absorption spectra at 10 mints intervals. In Fig. 9, the absorption peak at 400 and 550 nm corresponding to 2-NA shows slow reduction and disappearance after 150 minutes, respectively.
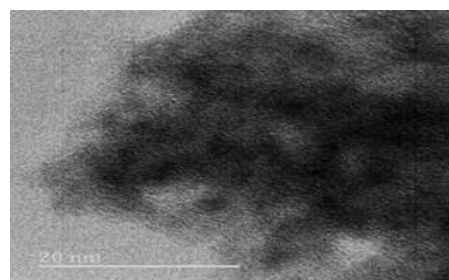
Fig. 7. HRTEM of $NiFe_2O_4$/IL/TiO_2 nanocomposite.
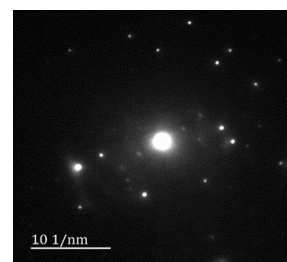
Fig. 8. Diffraction image of $NiFe_2O_4$/IL/TiO_2 nanocomposite.
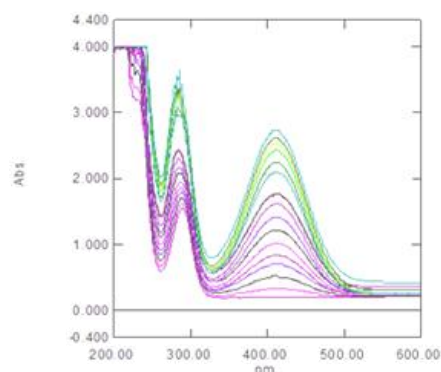
Fig. 9. UV spectrum for reduction of 2-nitroaniline.by $NiFe_2O_4$/IL/TiO_2 nanocomposite.

V. CONCLUSION

A nickel ferrite ionic liquid titanium dioxide ($NiFe_2O_4$/IL/TiO_2) nanocomposite was synthesized, characterized and applied to catalysis. The mass ratio of the nanocomposite is 2:1:1 of TiO_2, IL and $NiFe_2O_4$, due to the facilitation of interfacial charge transfer and inhibition of electron-hole recombination. The composite was successfully characterized by using SEM, EDS, TEM, HRTEM, DF and FT-IR techniques to identify the morphology, composition, crystallinity and important functional groups which are present in the composite. The advantage of this method is that it is an environmentally friendly safe protocol; less toxic, inexpensive and less harmful chemical are used; water is the solvent for the synthesis of nanocomposite under a green condition. In addition, it was easily recovered and re-used with negligible loss of catalytic activity. Moreover, the nanocomposite exhibited high catalytic activity for the reduction of 2-nitroaniline in water at room temperature.

REFERENCES

[1] B. Moghaddam, T. Nazari, J. Badraghi, and M. Kazemzad, "Synthesis of ZnO nanoparticles and electrodeposition of polypyrrole/ZnO nanocomposite film," *International Journal of Electrochemical Science,* vol. 4, pp. 247-257, 2009.

[2] M. R. Nabid, M. Golbabaee, A. B. Moghaddam, A. R. Mahdavian, and M. M. Amini, "Preparation of the -Al_2O_3/PANI nanocomposite via enzymatic polymerization," *Polymer Composites,* vol. 30, pp. 841-846, 2009.

[3] V. K. Vidhu and D. Philip, "Catalytic degradation of organic dyes using biosynthesized silver nanoparticles," *Micron,* vol. 56, pp. 54-62, 2014.

[4] N. Pradhan, A. Pal, and T. Pal, "Catalytic reduction of aromatic nitro compounds by coinage metal nanoparticles," *Langmuir,* vol. 17, vol. pp. 1800-1802, 2001.

[5] A. K. Sinha, M. Basu, S. Sarkar, M. Pradhan, and T. Pal, "Synthesis of gold nanochains via photoactivation technique and their catalytic applications," *Journal of Colloid and Interface Science,* vol. 398, pp. 13-21, 2013.

[6] M. Atarod, M. Nasrollahzadeh, and S. M. Sajadi, "Euphorbia heterophylla leaf extract mediated green synthesis of Ag/TiO_2 nanocomposite and investigation of its excellent catalytic activity for reduction of variety of dyes in water," *Journal of Colloid and Interface Science,* vol. 462, pp. 272-279, 2016.

[7] M. Nasrollahzadeh and S. M. Sajadi, "Synthesis and characterization of titanium dioxide nanoparticles using Euphorbia heteradena Jaub root extract and evaluation of their stability," *Ceramics International,* vol. 41, pp. 14435-14439, 2015.

[8] H. Liu, Y. Liang, H. Hu, and M. Wang, "Hydrothermal synthesis of mesostructured nano-crystalline TiO_2 in an ionic liquid–water mixture and its photocatalytic performance," *Solid State Sciences,* vol. 11, pp. 1655-1660, 2009.

[9] X. Y. Ma, Z. G. Chen, H. B. Jiang, J. Zou, and S. Z. Qiao, "Fabrication of uniform anatase TiO_2 particles exposed by {0 0 1} facets," *Chemical Communications,* vol. 46, pp. 6608-6610, 2010.

[10] S. Solinas, G. Piccaluga, M. P. Morales, and C. J. Serna, "Sol-gel formation of γ-Fe_2O_3/SiO_2 nanocomposites," *Acta Materialia,* vol. 49, pp. 2805-2811, 2001.

[11] S. C. Pang, S. Y. Kho, and S. F. Chin, "Fabrication of magnetite/silica/titania core-shell nanoparticles," *Journal of Nanomaterials,* 2012.

[12] Z. L. Shi, C. Du, and S. H. Yao, "Preparation and photocatalytic activity of cerium doped anatase titanium dioxide coated magnetite composite," *Journal of the Taiwan Institute of Chemical Engineers,* vol. 42, pp. 652-657, 2011.

[13] W. Fu, H. Yang, M. Li, M. Li, N. Yang, and G. Zou, "Anatase TiO_2 nanolayer coating on cobalt ferrite nanoparticles for magnetic photo catalyst," *Materials Letters,* vol. 59, pp. 3530-3534, 2005.

[14] M. Atarod, M. Nasrollahzadeh, and S. M. Sajadi, "Green synthesis of a Cu/reduced graphene oxide/Fe_3O_4 nanocomposite using Euphorbia wallichii leaf extract and its application as a recyclable and heterogeneous catalyst for the reduction of 4-nitrophenol and rhodamine B," *RSC Advances,* vol. 5, pp. 91532-91543, 2015.

[15] M. Nasrollahzadeh, "Green synthesis and catalytic properties of palladium nanoparticles for the direct reductive amination of aldehydes and hydrogenation of unsaturated ketones," *New Journal of Chemistry,* vol. 38, pp. 5544-5550, 2014.

[16] J. Lemus, J. Palomar, M. A. Gilarranz, and J. J. Rodriguez, "Characterization of supported ionic liquid phase materials prepared from different supports," *Adsorption,* vol. 17, pp. 561-571, 2011.

[17] C. Han, S. Ho, Y. Lin, Y. Lai, W. Liang, and Y. C. Yang, "Effect of stacking of water miscible ionic liquid template with different cation chain length and content on morphology of mesoporous TiO_2 prepared via sol–gel method and the applications," *Microporous and Mesoporous Materials,* vol. 131, pp. 217-223, 2010.

[18] L. W. L. Chang, B. Zhao, Z. Y. Gaosong, and S. W. Zheng, "Inorganic synthesis in ionic liquids," *Inorganic Chemistry,* vol. 47, pp. 1443-1452, 2008.

[19] I. Yavari, A. R. Mahjoub, E. Kowsari, and M. Movahedi, "Synthesis of ZnO nanostructures with controlled morphology and size in ionic liquids," *Journal of Nanoparticle Research,* vol. 11, pp. 861-868, 2009.

[20] E. Zarrin, N. Azizollah, S. Bahar, S. Bohlooli, and A. Banaei, "[PMIM]Br@TiO_2 nanocomposite reinforced hollow fiber solid/liquid phase micro-extraction: An effective extraction technique for measurement of benzodiazepines in hair, urine and wastewater samples combined with high-performance liquid chromatography," *Journal of Chromatography,* vol. B 980, pp. 55-64, 2015.

[21] A. Kale, S. Kale, P. Yadav, H. Gholap, R. Pasricha, J. P. Jog, B. Lefez, B. Hannoyer, P. Shastry, and S. Ogale, "Magnetite/CdTe magnetic-fluorescent composite nano-system for magnetic separation and bio-image," *Nanotechnology,* vol. 22, pp. 225101, 2011.

[22] D. Wang, L. Salmon, J. Ruiz, and D. Astruc, "A recyclable ruthenium (II) complex supported on magnetic nanoparticles: A region-selective catalyst for alkyne-azide cycloaddition," *Chemical communications.* vol. 49, pp. 6956-6958, 2013.

[23] F. Jing and S. Zhang, "Facile preparation of Fe_3O_4/mesoporous TiO_2 nanoparticles shell on polystyrene beads and its effective absorption of cyanobacteria in water," *Journal of Polymer Research,* vol. 22, pp. 182, 2015.

[24] A. Abbasil, D. Ghanbari, M. Salavati-Niasari, and M. Hamadanian, "Photo-degradation of methylene blue: photo-catalyst and magnetic investigation of Fe_2O_3-TiO_2 nanoparticles and nanocomposites," *The Journal of Materials Science: Materials in Electronics,* pp. 1-10, 2016.

[25] A. Allafchian, S. A. Hossein Jalali, H. Bahramian and H. Ahmadvand, "Preparation, characterization, and antibacterial activity of $NiFe_2O_4$/PAMA/Ag–TiO_2 nanocomposite," *Journal of Magnetism and Magnetic Materials,* vol. 404, pp. 14-20, 2016.

[26] Y. L. Pang, S. Lim, H. C. Ong and W. T. Chong, "Synthesis, characteristics and sono-catalytic activities of calcined c-Fe_2O_3 and TiO_2 nanotubes/c-Fe_2O_3 magnetic catalysts in the degradation of Orange G," *Ultrasonic Sono-chemistry,* vol. 29, pp. 317-327, 2016.

[27] Greene, R. Serrano-Garcia, J. Govan, and Y. K. Gun'ko, "Synthesis characterization and photocatalytic studies of cobalt ferrite-silica-titania nanocomposites," *Nanomaterials,* vol. 4, pp. 331-343, 2014.

[28] A. Vasanthakumar, I. Bahadur, G. G. Redhi, R. M. Gengan, and K. Anand, "Synthesis, characterization and thermophysical properties of ionic liquid N-methyl-N-(2´,3´-epoxypropyl)-2-oxopyrrolidinium chloride and its binary mixtures with water or ethanol at different temperatures," *Journal of Molecular Liquids.* Vol. 219, pp. 685-693, 2016.

[29] A. A. Ensafi, B. Saeid, B. Rezaei, and A. R. Allafchian, "Differential pulse voltammetry determination of methyldopa using MWCNTs modified glassy carbon decorated with $NiFe_2O_4$ nanoparticles," *Ionics,* vol. 21, pp. 1435-1444, 2015.

[30] A. A. Ensafi, B. Arashpour, B. Rezaei, and A. R. Allafchian, "Voltammetric behavior of dopamine at a glassy carbon electrode modified with $NiFe_2O_4$ magnetic nanoparticles decorated with

multiwall carbon nanotubes," *Materials Science and Engineering*, vol. 39, pp. 78-85, 2014.

[31] M. Anastasios, V. Tiverios, T. Christos, T. Nadia, B. Detlef, and D. Ralf, "Hydroxyapatite/titanium dioxide nanocomposites for controlled photocatalytic NO oxidation," *Applied Catalysis B: Environmental,* vol. 106, pp. 398-404, 2011.

[32] M. Mohamed, M. Mater, and M. Al-Esaimi, "Characterization, adsorption and photocatalytic activity of vanadium-doped TiO_2 and sulfated TiO_2 (rutile) catalysts: Degradation of methylene blue dye" *Journal of Molecular Catalysis A: Chemical,* vol. 255, pp. 53-61, 2006.

[33] M. Kooti and A. N. Sedeh, "Synthesis and characterization of $NiFe_2O_4$ magnetic nanoparticles by combustion method," *Journal of Materials Science and Technology,* vol. 29, pp. 34-38, 2013.

[34] W. Lan, C. Yan, Y. S. Lin, Y. N. Wang, F. Z. Yi, and P. C. Peng, "High efficient photo-catalyst of spherical TiO_2 particles synthesized by a sol-gel method modified with glycol," *Colloids and Surfaces A: Physicochemical and Engineering Aspects,* vol. 461, pp. 195-201, 2014.

[35] N. Sobana, M. Muruganadham, and M. Swaminathan, "Nano-Ag particles doped TiO_2 for efficient photo-degradation of direct azo dyes," *Journal of Molecular Catalysis A: Chemical,* vol. 258, pp. 124-132, 2006.

[36] J. Bandara, U. Klehm, and J. Kiwi, "Raschig rings-Fe_2O_3 composite photo catalyst activate in the degradation of 4-chlorophenol and Orange II under daylight irradiation," *Applied Catalysis B: Environmental,* vol. 76, pp. 73-81, 2007.

Vasanthakumar Arumugam is doing PhD under Prof. G. G. Redhi and Prof. R. M. Gengan in the Department of Chemistry. Durban University of Technology. He was born on January 19, 1988 in Tindivanam, Tamil Nadu, India. He studied the bachelor of science (BSc) in Govt. Arts and Science College in Tiruvannamalai. He studied his master's degree (MSc) in Bharathiar University Coimbatore. After his master's he has started carrier as a researcher (R&D) in SDS Ramcides Crop Science Pvt Lt. His early years of research focused on Agrochemical especially specialty fertilizers, pesticides, herbicides and plant growth regulators.

His research interests broadly focus on ionic liquids with their characterization and applications. His work also includes the use of aqueous based reactions and the preparation of nanoparticles and nanocomposites materials for industrial applications. His interest in nano-chemistry includes the use of ionic liquids and nanoparticle combinations and ionic liquid capped nanoparticles and magnetic nanoparticles for industrial and environmental applications. His recent research focus is synthesis, characterization and application of novel ionic liquids.

G. G. Redhi holds a PhD in chemistry from the University of Kwa-Zulu Natal, South Africa. The focus of his research work is on the determination of liquid-liquid equilibrium data for the separation of aromatic from aliphatic components related to the petroleum industry, using conventional polar solvents as well ionic liquids. In addition activity coefficients as well excess properties of binary and ternary systems are measured using chromatography and densitometry respectively. These thermodynamic data are important in optimizing solvent extraction processes, as well as lead to a better understanding of the molecular interactions that occur between the components.

In addition Prof Redhi's research also involves the use of nanotechnology, ionic compounds and new materials in the development of robust and sensitive electrochemical sensors for various active ingredients in the pharmaceutical industry, using Voltammetric techniques.

Robert M Gengan is an Associate Professor in the Department of Chemistry. Durban University of Technology. He was born on June 27, 1958 in Durban and from humble back-ground, he studied diligently and earned a lecturing position at the ML Sultan Technikon in 1985. He holds BSc, BSc (Hons), MTech, H.E.D and PhD degrees from the University Natal. His early years of research focused on Mycotoxin studies but later he turned towards chemistry; his major contribution in this field was the introduction of Environmental Chemistry II as an offering for the Higher National Diploma in Chemistry. In 2003, he introduced Green Chemistry in the Organic Chemistry IV syllabus and this still remains an interesting study component, which are enjoyed by students. His keen interest in Green Chemistry was highlighted in a Research paper titled "A New philosophical Approach to teaching: Green chemistry is the way of life" which was presented at the ICESA Conference in 2013. His lectures in organic chemistry is interspersed with updated Green Chemistry knowledge which stimulates creativity amongst students.

Trained as a synthetic organic chemist, Professor Gengan's research interests broadly focus on green chemistry with specific emphasis on synthesis of organic molecules by green protocols such as microwave irradiation and photo energy. His work also includes the use of aqueous based reactions and the preparation of less toxic nano catalytsts for industrial applications. His interest in nano-chemistry includes the use of indigenous plants to reduce gold, silver and palladium to nanoparticles capped with biomolecules for application on human health and the environment. His research team also uses active pharmaceutical molecules which are then linked to gold nanoparticles as an application for drug delivery systems. His recent research focus is the synthesis of fluorescent dyes and organic photo cells for the capture of solar energy. Professor Gengan hopes to add value to the environment by using Green Chemistry Principles in a systematic and holistic approach for challenges of sustainability of natural resources, of improving the environment thereby enabling a better quality of life.